

Automatic EEG analysis during long-term monitoring in the ICU

Rajeev Agarwal^a, Jean Gotman^{a,*}, Danny Flanagan^a, Bernard Rosenblatt^b

^aMontreal Neurological Institute, McGill University, 3801 University Street, Montreal, Quebec H3A 2B4, Canada

^bMontreal Children's Hospital, 3800 Tupper Street, Room A522, Montreal, Quebec H3H 1P3, Canada

Accepted for publication: 7 January 1998

Abstract

To assist in the reviewing of prolonged EEGs, we have developed an automatic EEG analysis method that can be used to compress the prolonged EEG into two pages. The proposed approach of Automatic Analysis of Segmented-EEG (AAS-EEG) consists of 4 basic steps: (1) segmentation; (2) feature extraction; (3) classification; and (4) presentation. The idea is to break down the EEG into stationary segments and extract features that can be used to classify the segments into groups of like patterns. The final step involves the presentation of the processed data in a compressed form. This is done by providing the EEGer with a representative sample from each group of EEG patterns and a compressed time profile of the complete EEG. To verify the above approach, 41 6 h EEG records were assessed for normality via the AAS-EEG and conventional EEG approaches. The difference between the overall assessment via compressed and conventional EEG was within one abnormality level 100% of the time, and within one-half level for 73.6% of the records. We demonstrated the feasibility and reliability of automatically segmenting and clustering the EEG, thus allowing the reduction of a 6 h tracing to a few representative segments and their time sequence. This should facilitate review of long recordings during monitoring in the ICU. © 1998 Elsevier Science Ireland Ltd. All rights reserved

Keywords: Prolonged EEG; Segmentation; Computer analysis; Intensive care unit; Clustering

1. Introduction

As with other modalities of monitoring in the ICU, the principal goal of neurological intensive care unit (ICU) EEG monitoring is to detect the onset of abnormalities at a reversible stage (Borel and Hanley, 1985). The EEG is an appropriate tool for monitoring because it provides a sensitive indication of cerebral metabolism, ischemia, hypoxia and neuronal dysfunction (Jordan, 1993). Other uses of EEG monitoring include the detection of subclinical seizures and extraction of information about the brain function in patients who have suffered severe nerve or neuromuscular junction disease such as the Guillain-Barre syndrome. The principal advantage of EEG over the clinical examination is that it is continuous and does not require patient cooperation.

Given some of the above advantages and the advent of

digital EEG recording, it is believed that EEG can and should be available in the ICU setting (Borel and Hanley, 1985; Emmerson and Chiappa, 1988). An EEG is particularly useful in providing a sensitive indication of cerebral functioning during periods when the brain is at risk. Such periods are often of long duration, hence a prolonged EEG recording may be required. Typically, a 16 channel, 24 h digital recording produces approximately 500 megabytes of data, the equivalent of over 8500 pages of conventional paper EEG. Review and interpretation of this raw EEG data is very tedious and time-consuming. A thorough review may require many hours of a neurologist's time. The advantage of computer analysis of prolonged EEG recordings is all too obvious.

Seizure and spike detection algorithms have been developed to identify epileptiform activity (see for example Gotman et al., 1979; Gotman, 1982; Gabor and Seyal, 1992; Harding, 1993), and only the portions of EEG containing spikes and seizures are stored for later viewing, thus achieving data selection during prolonged EEG monitoring. These detection methods present the neurologist with sections of

* Corresponding author. Tel.: +1 514 3981953; fax: +1 514 3988106; e-mail: jean@rclvax.medcor.mcgill.ca

EEG in the standard format, which are obviously not intended for background EEG assessment.

To address the problem of analysis of the EEG background during prolonged recording, several approaches have been proposed that compress and simplify EEG data. Bickford et al. (1971) introduced the Compressed Spectral Array (CSA) that presents the results of sequential spectral estimates of digitized EEG over time in an array. The display is generally limited to few hours of equivalent EEG and only for one or two channels (Bricolo et al., 1978), although modern CSA systems may be able to display more channels for longer periods of time. Trend analysis is another method of analyzing and presenting digitized EEG data. Labar et al. (1991) showed that the trend analysis of some parameters such as total power or alpha ratio revealed changes with subarachnoid hemorrhage prior to clinical manifestations. Maynard et al. (1969) introduced the Cerebral Function Monitor (CFM) that utilizes a single channel of EEG to produce integrated amplitude on paper in real-time. Discontinuity detection, with specific relevance to neonatal EEGs has been developed by Wertheim and colleagues (Wertheim et al., 1991, 1994) for an on-line analysis of EEG with a reduced electrode coverage. This system determines the amount of discontinuity in a recording and the RMS amplitude, then displays these on a compressed time axis. In one form or another, all these methods provide a display of processed information that require training and experience for proper interpretation.

Given the various shortcomings of these methods, none have found common usage in the ICU setting. In this paper, we present a new method of computer analysis of prolonged EEG recordings. We have developed a systematic approach for automatic EEG analysis that relies on the observation that the background activity in a long-term EEG usually consists of different patterns that are recurrent. In a normal EEG, for example, these patterns may relate to the cycling of the sleep stages; in post-operative recovery EEG, they may relate to different levels of vigilance. Although there is a possibility of numerous patterns in different patients, only a few types of EEG patterns are usually present in the prolonged EEG record of a particular patient (Barlow et al., 1981). This leads to the idea of recurrence of different EEG types in the recording. In this paper, we present the method of decomposing the EEG into recurrent types. This is a 4 step process. We first describe the signal processing procedure to break down the multichannel EEG into stationary segments. After eliminating any segments clearly contaminated by artifacts, the second step involves the extraction of features that describe each EEG segment as a point in n -dimensional space. Along with the classical amplitude measure, a new measure of the 'central' frequency and a new frequency-weighted energy measure are described. The third step involves clustering of the segments based on the features extracted in step two. This is accomplished by developing an ad hoc procedure using the k -means clustering algorithm as a building block. This algo-

rithm and its important features are presented as the third step in the procedure. Special attention is given to the detection and elimination of artifactual segments. As step 4, we describe how the results can be used to display compressed, prolonged EEG in two pages.

This basic 4 step strategy has been applied to integrate the analysis of prolonged EEG recordings into the Automated Analysis of Segmented EEG (AAS-EEG) technique. The idea is not to replace the complete EEG but to supplement it with a compressed version that can be used to give rapidly an overall assessment of the background activity. The compressed display includes representative samples of the different types of background present in the recording, shown as a traditional EEG, as well as a graph representing its temporal organization. The resulting output is only a few pages even for a 24 h recording and can be faxed or transmitted via modem to the neurologist by the ICU staff for a quick review, hence providing timely dissemination of information for better patient care. Within each of the above 4 steps, several new ideas are developed. Additionally, we will present the results of a validation of the AAS-EEG technique using EEGs obtained from children immediately after cardiac surgery.

2. Methods

2.1. Adaptive segmentation based on nonlinear energy operator

The EEG is a non-stationary signal and for any automatic analysis system, it is essential that it be broken into sections that are of similar type. This involves segmenting the EEG into quasi-stationary sections and can be achieved by drawing a boundary at the instants where there is a change in the EEG pattern, for example, alpha blocking following eye opening.

In Agarwal and Gotman (in preparation), a new technique to segment the EEG into quasi-stationary sections has been presented. This procedure has minimal need for parameter adjustment. For completeness, we briefly review this new segmentation strategy.

In his work on nonlinear speech modeling, Teager proposed a simple nonlinear energy operator (NLEO) (Ψ_{kaiser} , given here (as presented in Kaiser, 1990) in its discrete form as

$$\Psi_{\text{kaiser}}[x(n)] = x^2(n) - x(n-1)x(n-2) \quad (1)$$

One of its key properties for a pure sinewave can be summarized by the rule

$$\Psi[\text{Acos}(\omega_0 n + \theta)] = \frac{1}{2} A^2 \omega_0^2 \quad (2)$$

Clearly, examining Eq. (2), the output is proportional to both amplitude and frequency and has been termed frequency-weighted energy.

Plotkin and Swamy (1992) presented a more generalized form of the NLEO

$$\Psi_g[x(n)] = x(n-l)x(n-p) - x(n-q)x(n-s) \quad l+p=q+s \quad (3)$$

It can easily be shown that for $l \neq p$ and $q \neq s$, Ψ_g is more robust to noise. That is, if the input signal x contains additive white noise, then the output in Eq. (3) will not contain a component reflecting the input noise. This is due to the removal of the square term in Eq. (3). For this reason we have chosen to use $l = 1$, $p = 2$, $q = 0$ and $s = 3$ to detect the changes of stationarity in a signal. These changes or segment boundaries can be detected by using a sliding temporal window method (Krajca et al., 1991) as shown in Fig. 1. For a given time instant, n , the frequency-weighted energy in the left half of the window is subtracted from that of the right half of the window to generate the signal $G_{\text{nleo}}(n)$ as shown in Fig. 1. Mathematically, the signal $G_{\text{nleo}}(n)$ can be written as

$$G_{\text{nleo}}(n) = \sum_{m=n-N+1}^n \Psi(m) - \sum_{m=n+1}^{n+N} \Psi(m) \quad (4)$$

where the window size is $2N$ samples in duration.

If the two half-windows have the same energy, the resulting signal $G_{\text{nleo}}(n)$ is zero; if the window is centered at a discontinuity (segment boundary) then $G_{\text{nleo}}(n)$ is large. Therefore, the time instants of the local maxima in the signal $G_{\text{nleo}}(n)$ may be taken as the segment boundaries.

The segmentation criterion $G_{\text{nleo}}(n)$ generates some spur-

ious segment boundaries due to inherent random fluctuations. The number of these redundant boundaries can be reduced by applying a thresholding to the segmentation criterion. One adaptive threshold procedure is suggested by the following

$$T(n) = \begin{cases} \max[G_{\text{nleo}}(n-L/2 : n+L/2)] & \text{for } n=L/2, (L/2+1)\dots \\ 0 & \text{for } n=0, 1, \dots, (L/2-1) \end{cases} \quad (5)$$

By applying $T(n)$, a new segmentation criterion can be derived,

$$G(n) = \begin{cases} G_{\text{nleo}}(n) & \text{if } G_{\text{nleo}}(n) \geq T(n) \\ 0 & \text{if } G_{\text{nleo}}(n) < T(n) \end{cases} \quad (6)$$

Final segmentation boundaries can be detected by finding the local maxima or peaks in either $G_{\text{nleo}}(n)$ or its thresholded version Eq. (6). In this work, we have used the thresholded version of the $G_{\text{nleo}}(n)$. Multichannel EEG recordings can be handled by grouping channels corresponding to anatomical regions:

$$G_{\text{nleo}}^T = G_{\text{nleo}}^1 + G_{\text{nleo}}^2 + \dots + G_{\text{nleo}}^P \quad (7)$$

where G_{nleo}^i , $i = 1, 2, \dots, P$ represent the segmentation criterion for each of the P channels in any group. Fig. 2 provides an example of multichannel segmentation for channels of the left hemisphere. In this example and all subsequent segmentation, we have forced the minimum duration of a seg-

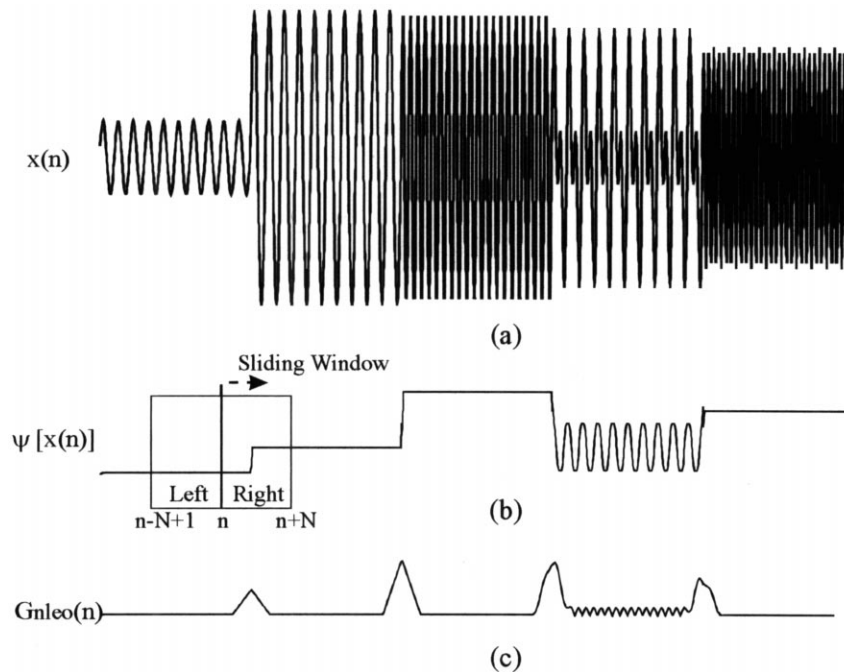


Fig. 1. Application of the proposed segmentation method emphasizing its utility in detecting frequency or amplitude changes in the input signal. (a) Simulated input signal. (b) Output of the NLEO. (c) NLEO-based segmentation criterion.

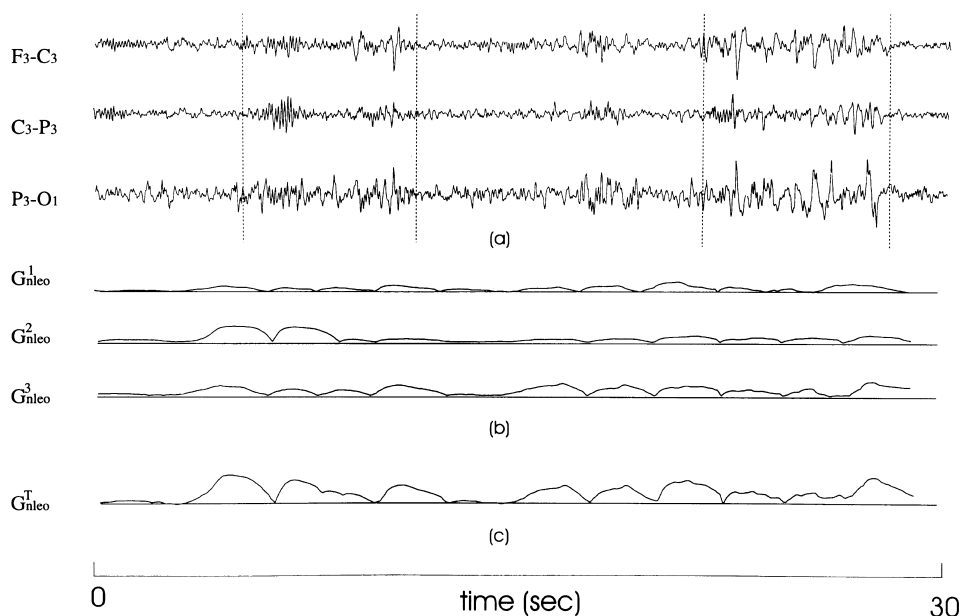


Fig. 2. Example of multichannel segmentation based on the NLEO segmentation criterion. (a) Three channel input signal. (b) Segmentation criterion for each channel in (a). (c) Overall multichannel segmentation criterion for all 3 channels.

ment to be 3 s. In the detection of local maxima, any detection that generates a segment of duration less than 3 s was not considered as a segment boundary.

Minimum segment duration was chosen to be 3 s to limit the number of segments generated due to transient phenomena. The aim of the method is primarily to aid in assessing the background EEG. It is assumed that transient information is extracted with other methods. Arbitrary segment duration will generate a much larger number of segments of short duration. This may make the algorithm computationally prohibitive. Furthermore, features extracted from relatively small segments may not be representative of the segment. A minimum duration of signal is required in order for the features to be meaningful. On the other hand, by forcing the minimum duration to be 3 s we lose the ability to explicitly identify features such as spindles and K-complexes, thus affecting the time-variability assessment of the EEG.

It is obvious that there exists a tradeoff in choosing the minimum segment duration. For the post-operative EEGs considered in this work, a minimum segment duration of 3 s was found to be a good compromise.

2.2. Feature extraction

The second step in the proposed AAS-EEG approach is the extraction of a feature vector that is representative of each EEG segment generated in the first step.

In an attempt to describe the temporal and spectral characteristics of EEGs, numerous features have been described by many researchers. Some examples include average amplitude, variability of amplitude, maximum and minimum value of amplitude, first and second derivatives, and amplitudes in different spectral bands (Creutzfeldt et al.,

1981; Krajca et al., 1991; Pietela et al., 1994). In our method, we use 3 features per channel to describe each segment: a measure of amplitude, a measure of frequency and the frequency-weighted energy based on the NLEO idea. Before discussing these measures, we first present the initial strategies applied for artifact rejection.

2.2.1. Artifact rejection

Automated identification and elimination of artifact contaminated EEG is a difficult problem in any type of analysis. In the self-organization or clustering of the EEG segments, it is particularly troublesome. To combat this, we made special efforts in its identification and applied the following 3 strategies for the elimination of artifact contaminated segments.

Maximum amplitude threshold. We eliminated any segment where the absolute maximum amplitude in any channel of any segment exceeds a fixed threshold. This threshold was chosen to be $300 \mu\text{V}$. Background EEG signals usually do not exceed this value. We realize that this may result in the elimination of some epileptiform activity, but this analysis is aimed at the background activity and assumes that epileptiform transients, spikes and seizures, are handled by a separate approach.

Frequency-weighted energy. Some artifact such as muscular activity will pass through amplitude screening. To overcome this, we used an ad hoc technique based on the distribution of the frequency-weighted energy measure for each channel. Since this energy is proportional to amplitude and frequency, the increased frequency or amplitude due to muscular artifacts forces the energy to be farther away from the actual EEG energy. Furthermore, since most of the segments are actual EEG, the collection of the energy points will be denser in the energy space corresponding to EEG

than the artifacts. Empirical observations confirm that the points on the extreme edges of the frequency-weighted energy distribution are isolated and often contain artifacts. We, therefore, used the measure of energy distribution as an artifact detector. An original aspect of this approach is that we use a dynamic threshold that depends on the density of the frequency-weighted energies for each of the channels in the segments.

Contralateral EEG. Another means of detecting artifact contaminated EEGs is to automatically eliminate all segments corresponding to times at which the contralateral EEG has been considered to be artifactual. We assume that if there is an artifact on one side, then the other side has some form of artifact as well. However, in the event that there is no artifact on the considered side, some genuine EEG will be eliminated. This does not pose a great problem in the prolonged EEG: in comparison to the amount of available data, the loss of some non-artifactual data does not influence the AAS-EEG results to a great extent.

2.2.2. Amplitude measure

The amplitude measure is simply the average amplitude over a segment. Let $x_j(n)$ be the segment under consideration, where j is the segment number, then the average amplitude for each channel in the j th segment is determined as

$$A_{ij} = \frac{1}{M_j} \sum_{n=1}^{M_j} |x_{ij}(n)| \quad i=1, 2, \dots, P \quad (8)$$

where M_j is the number of points in j th segment and i is the channel number.

2.2.3. Frequency measure

Many researchers have attempted to define some representative measure of average frequency; however, there is no consensus on a good measure. One such measure has been recently described by Krajca et al. (1991)

$$FDIFF = \sum_{n=1}^{M_j} |x_{ij}(n+1) - x_{ij}(n)| \quad (9)$$

where M_j , j and i are as in Eq. (8). It can easily be shown (Wendling, 1996) that Eq. (9) is inadequate in representing the spectral characteristic of the EEG. We present a new measure that, in some ways, describes the central frequency tendencies of the EEG segment. Given a signal modeled by an Autoregressive (AR) model of order P ($P > 2$), it may be possible to track the central frequencies by the coefficients of a reduced order model. The hypothesis is that the reduced (or insufficient) order AR model will compensate for higher model order by fitting the signal in a manner that reflects its power distribution (i.e. amplitude at different frequencies). Specifically, the frequency value derived from the estimated AR coefficients of a second order model is affected by the relative power of each frequency component in the input signal. We may therefore consider it to represent the frequency content of the signal. Although central frequency connotes a specific meaning, we have

used this term here to describe the new measure of frequency. Fig. 3 illustrates this measure using simulated data.

Fig. 3a shows that when the input signal spectrum has only one peak, it is well modeled by a second order AR model and the estimate of the frequency is exact. Fig. 3b shows the spectra of a simulated signal with several peaks. In this case, the estimated central frequency is 3.6 Hz in the neighborhood of 3 Hz (the frequency with maximum power). The second order AR model did not lock onto this 3 Hz peak, but instead modeled the overall spectrum as can be seen by the dashed curve. The central frequency reflects the existence of frequencies other than the dominant 3 Hz.

In Fig. 3c, we add a higher frequency component to the signal of Fig. 3b and see that the estimate of central frequency is skewed to the right to reflect the addition of this signal component. Similarly, in Fig. 3d we increase the power of the additional higher frequency component. This causes the central frequency to be further skewed to the right in response to the additional power at a higher frequency.

2.2.4. Frequency-weighted energy measure

The third feature used to describe the EEG segments is the frequency-weighted energy as calculated by the expected value of the output of the nonlinear energy operator. It can be calculated using Eq. (2) where Ψ is described by Eq. (3). This energy is different from *mean-square energy* as it reflects the frequency as well as the amplitude content of a signal. Amplitude and rhythmicity are both used in the visual EEG evaluation. The frequency-weighted energy, determined by the NLEO, inherently combines both of these notions into a single measure. As such, we feel that the resulting frequency-weighted energy is different from frequency or amplitude features and should be used as an additional feature in the proposed AAS-EEG technique.

2.2.5. Multichannel feature vector

The feature vector, f_i , consists of 3 features for each channel, namely, the amplitude, central frequency and the frequency-weighted energy. In the multichannel case, we generate a larger feature vector with $3P$ entries by concatenating the feature vectors of each channel within the segment

$$F_j = [f_{1j} | f_{2j} | \dots | f_{Pj}] \quad (10)$$

where the subscript ' j ' represents the segment number and P the number of channels.

2.3. Classification of the segmented EEG

The third step in the AAS-EEG analysis is the classification of the segments generated in step one into groups that are of similar types. This was first attempted by Bodenstern and Praetorius (1977) using Ward's hierarchical clustering

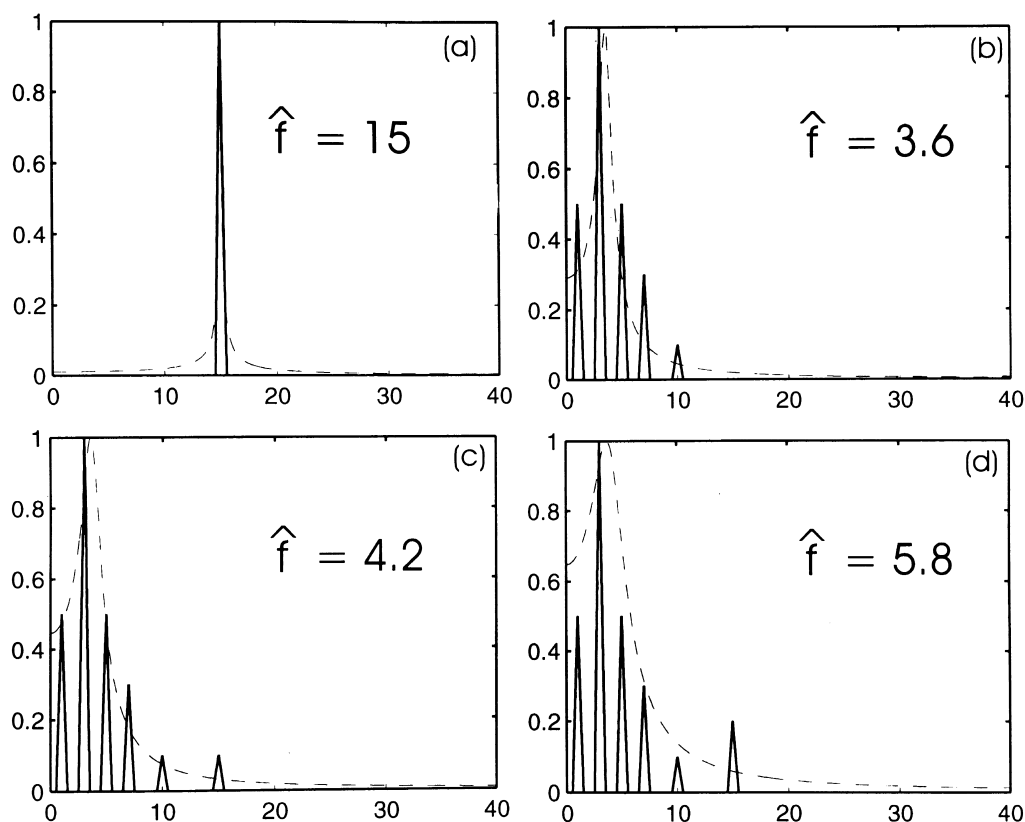


Fig. 3. Illustration of the frequency measure of central frequency based on the second order AR model. (a) AR model order matches the order of the signal. Frequency estimate is exact. (b) AR model order much less than the signal order. Frequency estimate does not match any of the signal components, but models the central frequency. (c) Same as in (b), but with an additional higher frequency component. Frequency estimate increases to compensate for the additional energy at higher frequency. (d) Same as in (c), but with an increased power in the additional higher frequency component. Frequency estimate increases to compensate for the increased power.

method (Ward, 1963). Other investigators have tried the probabilistic approach (Bodenstein et al., 1985), fuzzy cluster analysis (Amir and Gath, 1989; Krajca et al., 1991) and variant of *k-means* clustering algorithms (Sanderson, 1980). In all work to date, classification of EEG segments has been restricted to short duration EEG. In contrast, in the current approach, we are applying it to prolonged EEGs. To do so, we have chosen to use the *k-means* clustering algorithm for classification of the feature vectors (Eq. (10)) corresponding to the segments.

The aim of the basic *k-means* algorithm is to categorize or divide J objects with n dimensions (in the current application the J feature vectors corresponding to the J segments with $3P$ dimensions) into k groups or clusters such that, the within-cluster sum of distances between member points and the centroid is minimized. In general, the globally optimal solution for large values of J , n and k is not feasible, hence a locally optimal solution is sought. In implementing the *k-means* algorithm, two key difficulties are encountered: (1) the lack of a priori knowledge of the number of natural clusters in the data, and (2) the seed values for cluster centroids.

Further, in the computer analysis of EEG, the identification and elimination of artifactual segments is generally a

difficult problem. This becomes even more problematic in the clustering stage. To deal with these we have developed an ad hoc clustering procedure based around the *k-means* algorithm. We have made a special effort in identifying and eliminating EEG segments contaminated with artifacts that were not eliminated by the strategies described earlier. This greatly improves the clustering process and the results of the AAS-EEG procedure. Table 1 describes the steps in the algorithm.

The general strategy in our classification procedure revolves around iterative clustering. First, we organize the feature vectors into a number of clusters that exceeds the number of presumed or natural clusters within the data. By natural, we mean clusters in which there is a clinically relevant differentiation of the EEG segments. It is expected that some of the extra clusters will correspond to EEG that has no clinical value (i.e. possibly segments containing remaining artifacts), while others may be redundant clusters generated by splitting genuine clusters. In the second stage of our clustering procedure, having eliminated the unwanted EEG segments that can significantly influence clustering, we recluster the data using the exact number of desired clusters. If it is suspected that some artifact contaminated EEG segments still prevail, then this strategy can

Table 1

Clustering strategy for m-channel segments

Step 1	Set initial parameters
1.1	k_f , final number of clusters desired
1.2	k_i , initial number of clusters to start with
1.3	T_{merge} , cluster merging criterion. A percentage of average inter-cluster distance
Step 2	Adjust/scale volume of feature space
Step 3	Find initial, k_i , seeds for clustering
Step 4	Cluster using <i>k-means</i> algorithm
Step 5	Find outlier clusters. Eliminate all members belonging to these clusters
Step 6	Separate remaining clusters into two groups using T_{merge} criterion
Step 7	In each of the two groups generated in the last step, merge clusters that are too close together using a user supplied fraction of average inter-cluster distance
Step 8	Readjust/rescale volume of feature space to accommodate the elimination of outliers
Step 9	Using the centroids of current valid clusters as candidate seeds, determine k_f seeds for final clustering
Step 10	Recluster using <i>k-means</i> algorithm
Step 11	Remove outliers clusters, if any

always be applied iteratively. In our experience with the algorithm, this was not necessary as it did not greatly improve the results. The following provides a brief description and reasoning for the key steps in the clustering procedure of Table 1.

2.3.1. Initial parameters

Some key parameters must be initialized at the start of clustering. The first is the number of clusters, k_f , or the number of different types of EEG patterns that are expected in the data. While the number of possible EEG patterns is large, Barlow et al. (1981) suggested that the number of actual patterns in a single record can be expected to be 5 or fewer. For this reason we have chosen $k_f = 5$. Experimenting with the post-operative EEGs used in this work confirms that $k_f = 5$ is an appropriate choice. The second parameter is the number of clusters with which to start, k_i , that must be larger than k_f to accommodate any artifactual EEG. We have chosen to use $k_i = 9$. Our own experimental evidence suggests that most of the artifactual EEG can reasonably fit into 3 or 4 clusters. The third parameter is the threshold, T_{merge} , which is used to merge clusters that are too close together. This is defined as a percentage of inter-cluster distance. A description of the inter-cluster distance is given later in this section. By experimenting with the procedure we have settled on $T_{\text{merge}} = 40\%$. There is no ideal way of choosing this parameter since the merging of clusters is generally a difficult problem and empirical adjustment must be used.

2.3.2. Seeds for clustering

The *k-means* algorithm requires initial seed points (clus-

ter centroids) around which clustering is performed. Several methods (Anderberg, 1973) of choosing the seeds have been suggested but no optimal approach exists. In our experience, the choice of initial seed points is very critical in order for the algorithm to converge to a reasonable solution. We have used a variation of the method described in Anderberg (1973).

The initial set of k_i seed points can be found by using some of the actual data points as the seed points. First a large number of data points, k ($k > k_i$) are randomly selected thus allowing a good representation of the different EEG types present in the record. Next, we reduce the k seeds to k_i as follows: Let d_{xy} be the distance between any two candidate seeds, k_x and k_y . We reduce the k candidate seeds to $k - 1$ by replacing the two seeds having the minimum d_{xy} by their arithmetic average. By continuing this process iteratively, the k candidate seeds can be reduced to the desired k_i seeds. In this way, we ensure that the initial set of seeds are in regions that represent different EEG types.

2.3.3. Cluster merging

After the initial redundant clustering, it is necessary to reduce the k_i clusters to the desired number of k_f final clusters. This is the objective of steps 5 through 7 in the algorithm of Table 1. These steps involve the elimination or merger of clusters after the initial clustering has been performed. First, any cluster containing fewer than a prespecified number of members (N_{out}) is considered as an outlying cluster and removed from any further processing. In this paper, we used $N_{\text{out}} = 0.5\%$ of the total number of segments. The corresponding EEG segments are placed in the artifact category. It is possible that such segments contain clinically relevant transient information; however, our intention here is to assess the background EEG. Other methods are available for the detection of rare events. With respect to the background assessment there may be a loss of less than 0.5% of the total number of segments in the record.

The next step is to separate the remaining clusters into two groups. The idea is to isolate clusters that are far away from the majority of clusters. We want to minimize the dominance of any remaining outlying clusters in the cluster merging process. We do this by placing all clusters with an inter-cluster distance greater than 2 standard deviations of the mean distance into one group; while the remaining clusters form the second group. The inter-cluster distance is defined as the mean of the distances from the considered cluster centroid to all other cluster centroids in the set. The clusters within the two formed groups can then be merged independently to eliminate redundant clusters. To do this we have developed a cluster merging algorithm that depends on the inter-cluster distance and a merging criterion, $T_{\text{merge}} = 40\%$.

The following algorithm can be used to merge clusters that are too close together. Let $d(k_x, k_y)$ be the Euclidean distance between the centroids of clusters k_x and k_y and \bar{d} be the average distance between all pairs of cluster centroids. If

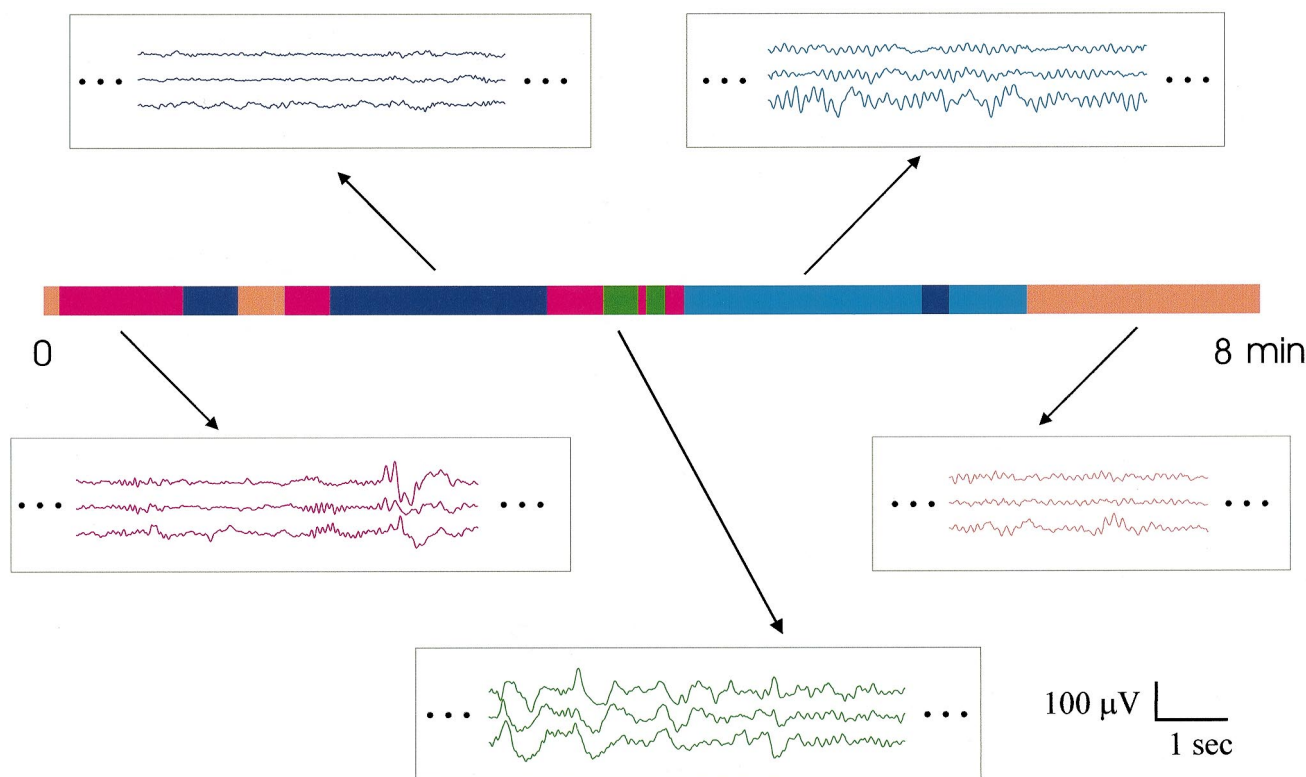


Fig. 4. Illustration of the time evolution of different EEG types for an 8 min segment.

$$\min(d(k_x, k_y)) < \frac{T_{merge} \bar{d}}{100}$$

then merge the k_x and k_y clusters

$$k_x \cup k_y \rightarrow k_x$$

Repeat until the above criterion is not satisfied.

2.4. Display of compressed EEG for clinical use

The effectiveness of the AAS-EEG is dependent on its presentation. The output of AAS-EEG is displayed in two components. The first one displays a representative segment from each of the 5 clusters. We have chosen to display the segments closest to the cluster centroids. The second component consists of chronological sequence of EEG patterns (time profiles) that has been color coded to relate each segment to a particular cluster. The duration of each segment on the time profile is proportional to the duration of each EEG segment in real time.

These two components of the AAS-EEG can be used to provide a description of the prolonged EEG. Fig. 4 shows an 8 min portion of a time profile and relates the colors to different patterns in the record. For example, the occurrence of the first blue segment represents the EEG pattern described by Type 5 activity. Thus, all subsequent occurrence of blue will represent the same type of EEG pattern.

To provide some anatomically relevant information the AAS-EEG technique can be applied to multichannel record-

ings that are grouped corresponding to anatomical regions. In our case, we formed two groups, one for the left hemisphere and one for the right. We thus have two sets of clusters and two time profiles of the EEG — one for each hemisphere. This provides some information regarding symmetry. We, therefore, have chosen to provide the clinician with a summary consisting of two pages. The first page provides a representative EEG segment for each type of pattern for each side. In the representative segment displayed for each type, we have also included the contralateral EEG. This provides the EEGer with extra information about EEG symmetry. The second page provides two time profiles, one for each side of the brain, describing how the EEG changes over time. Thus, the time profile consist of an hour-by-hour dual horizontal line — one for the left and one for the right hemisphere. Figs. 5a and 6a show an example of the AAS-EEG output.

Where possible, we attempted to match the colors in the time profile so that the same color represents similar EEG types on both sides of the brain. This is generally a difficult problem when the basis of cluster distinction is waveform morphology. Color matching was attempted by comparing temporal distribution of each EEG type in the right and left hemisphere.

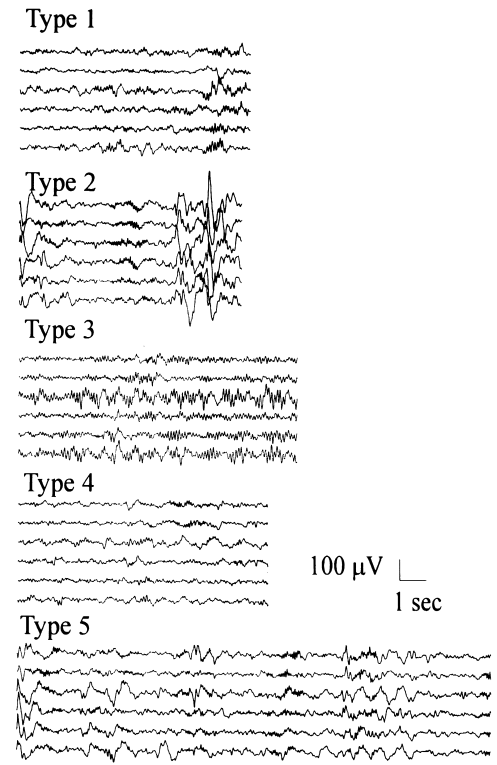
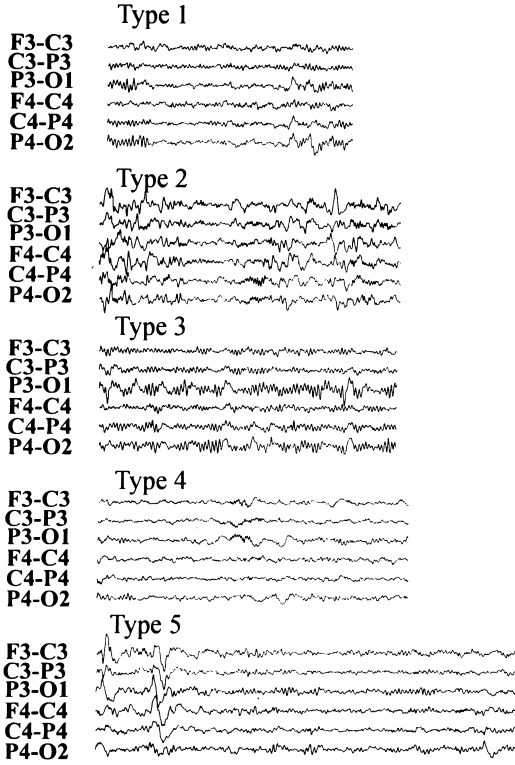
2.5. Validation

The proposed AAS-EEG technique compresses prolonged EEG into a two-page summary that can assist in

5

(a) Left Side EEG Types

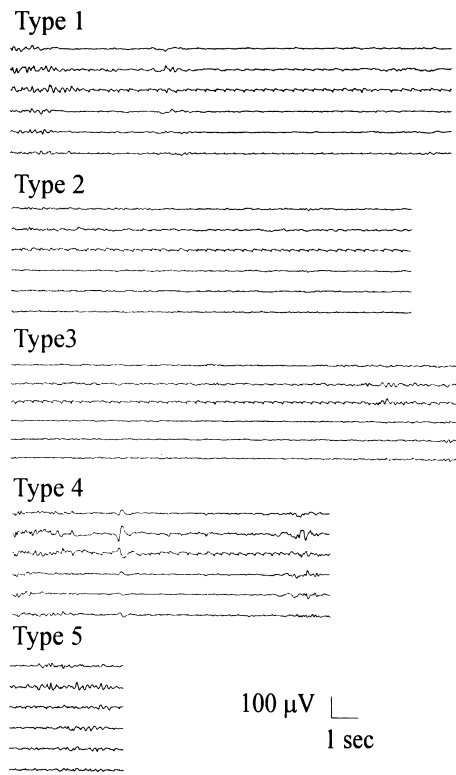
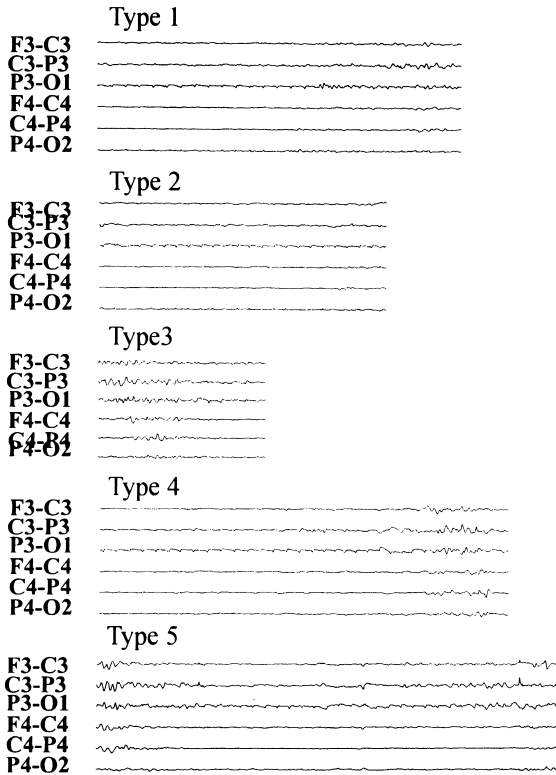
Right Side EEG Types



Filename: TOK150C2

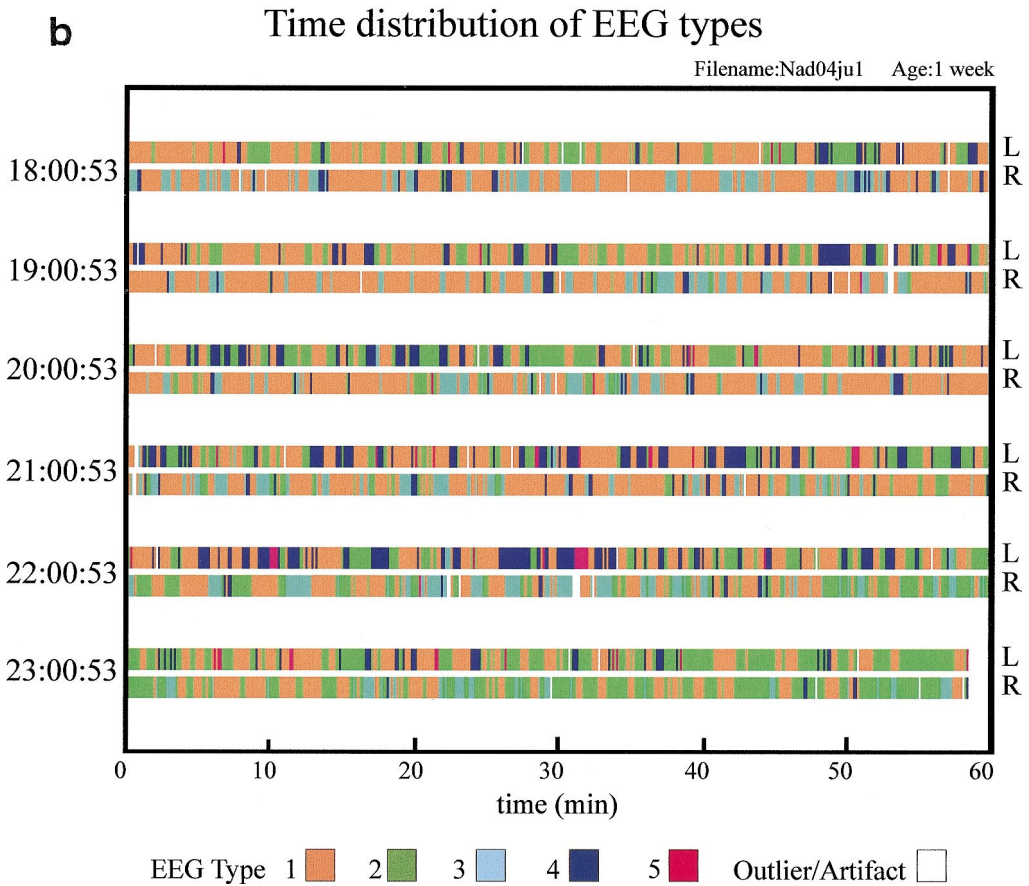
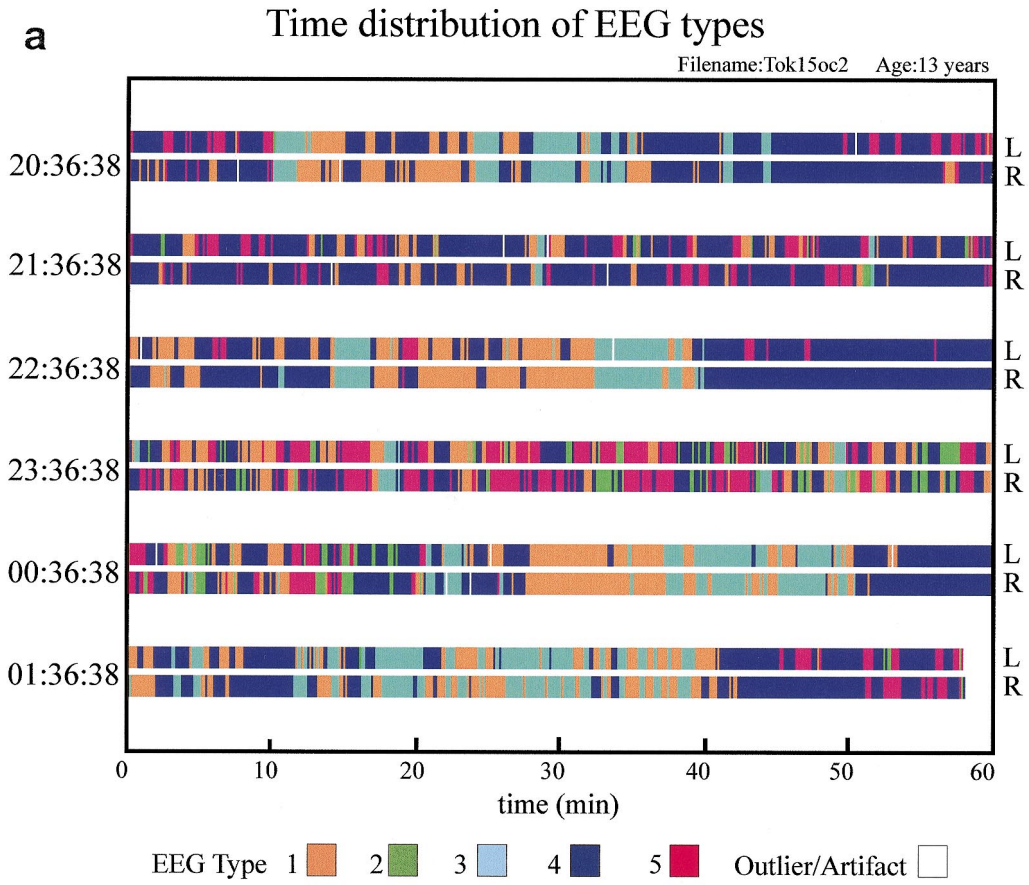
(b) Left Side EEG Types

Right Side EEG Types



Filename: NAD04JU1

6



providing a general assessment of the background EEG. We evaluate the performance and usefulness of the AAS-EEG approach with the following validation protocols.

2.5.1. Initial EEG review

Two hundred thirty-seven 6 h sections of EEG, obtained from 90 children following cardiac surgery, had been reviewed by one of the authors for a previous study (Si et al., in press). The age distribution of the children was from newborn to 10 years. The EEGs were recorded in an 8 channel bipolar montage (F3-C3, C3-P3, P3-O1, F4-C4, C4-P4, P4-O2, T3-Cz, T4-Cz). These EEG sections were assessed based on a review of the first 15 min in every hour to quantify various features of the background, along with any events considered significant and labeled by the recording technician. The following features were quantified: amplitude, symmetry, time variability and overall background. Each feature was assessed according to 7 categories: normal, normal to mildly abnormal, mildly abnormal, mildly to moderately abnormal, moderately abnormal, moderately to severely abnormal and severely abnormal. This provided a database of pre-assessed EEGs that could be re-evaluated using the proposed AAS-EEG procedure.

The above classification of EEGs into 7 categories is currently in use in our laboratory. Of course, other clinicians may use a coarser classification scheme. The classification of EEGs is only used to assess the performance of the AAS-EEG approach. Whether it is detailed or coarse, it does not influence the actual method since it only serves to evaluate performance. If a less detailed classification is used, an improved performance of the AAS-EEG method should be expected.

2.5.2. Review of AAS-EEG generated compressed EEG

Forty-one 6 h sections were chosen randomly from the reviewed records. The output of the AAS-EEG was then reviewed by one EEGer who was informed only of the age of the patient. To minimize the chance of reviewer bias due to the initial review of the complete EEG, the patient name was removed from the compressed EEG and an 8 month period elapsed between the initial EEG review and the current evaluation. Despite our attempts in minimizing reviewer bias, it should be noted that EEGers can often recognize interesting EEGs based on particular patterns. Given that only selected sections were presented, we believe this is not a major problem. The compressed EEG consisted of two representative segments of each EEG cluster as determined by the classification stage and two 6 h time

profiles (one for each hemisphere) describing the time evolution of the EEG. The representative EEG segments for each type were the two segments closest to each cluster centroid and lasting more than 7 s. It should also be noted that representative segments included the EEG from both hemispheres, even though they represent the EEG type of only one side. Bilateral EEG was presented to assist in evaluating symmetry.

The compressed EEG was then reviewed according to various features. Amplitude and symmetry were assessed based on the representative samples. Time plots were used to identify the onset and offset of periods of asymmetry. Time variability was assessed according to age-dependent sleep feature identification. The time plots were used to confirm that the identified features changed in an appropriate manner and also to locate periods of any paroxysmal events.

In addition, an assessment of improvement, stability or worsening of the EEGs was made based on the combined information provided by the time plots and the segments representing different types of EEGs. Any other characteristic extracted from the compressed data was noted.

Assessment for each feature and the overall background EEG were then tabulated and compared to the results obtained from the conventional review method using a contingency table. Percentage of agreement on the abnormality scale, described earlier, was computed. Four different values were computed: complete agreement, agreement to within one half-level, agreement to within one level and agreement beyond one level.

3. Results

We present two examples of the compressed EEG obtained by applying the AAS-EEG technique. These serve two purposes: first they show typical compressed EEGs for a record where the EEG is relatively unchanging in one, while there are clear changes in the other. Second, we use them to describe the differences in the time profiles for different EEG records. Figs. 5a and 6a show the compressed version of a record that contains 5 clear patterns (EEG types). Fig. 5a shows the representative segments for each of the clusters in the left and right hemispheres and Fig. 6a shows the time profiles of these segments. Examining the time profile, it is clear that there is an agreement in the time variability of the EEG pattern between the left and right hemispheres. Matching of the left and right

Fig. 5. (a) Example of the output of the AAS-EEG technique for a 6 h section of EEG in which there are clear changes in EEG patterns. Representative EEG types present in the two hemispheres. All five clusters in the two hemispheres have been matched so that the numbered EEG types represent the same types of EEG on the two sides. (b) Example of the output of the AAS-EEG technique for a 6 h section of EEG in which there is no clear clinical time variability. Representative EEG types present in the two hemispheres. In this case the cluster matching resulted in only one cluster that matched. This is primarily due to splitting of natural clusters (thereby, the randomness in the cluster assignment).

Fig. 6. (a) Time profile of the EEG for the two hemispheres shown in Fig. 5a. (b) Time profile of the EEG for the two hemispheres shown in Fig. 5b.

Table 2

Overall assessment

		Compressed EEG review						
		Norm	Norm-Mild	Mild	Mild-Mod	Mod	Mod-Sev	Sev
Conventional	Norm	8	1	5	0	0	0	0
EEG review	Norm-Mild	4	1	1	0	0	0	0
	Mild	3	0	4	1	0	0	0
	Mild-Mod	0	0	0	2	1	0	0
	Mod	0	0	1	0	2	2	0
	Mod-Sev	0	0	0	0	0	1	0
	Sev	0	0	0	0	2	0	0

Norm, normal; Mod, moderate; Sev, severe; Mod-Sev, moderate to severe.

side EEG time profiles (i.e. cluster matching) resulted in all 5 clusters on the two sides being matched. This indicates that all 5 EEG types in this record are distinct and there is a good likelihood that there is no asymmetry in this record. It should be noted that the time profiles in the two hemispheres are not time-locked because the EEGs of the two hemispheres were segmented and analyzed independently.

Figs. 5b and 6b show the results of applying the AAS-EEG technique to an undifferentiated EEG record, as illustrated by the similarity of the patterns in Fig. 5b. In this record, we have at most two EEG pattern types. Thus, by splitting the segments into 5 clusters, we force some randomness in their organization, resulting in a poor agreement between the time profiles of the two hemispheres (Fig. 6b). Since the analysis of the two hemispheres was done independently, it is expected that the two time profiles will show a poor agreement in time distribution of the segments. However, by using the representative segments and time profiles, it is still possible to make an adequate decision as to the normality of the record. Moreover, cluster matching resulted in only one cluster that matched in the time distribution on both sides. Examining the time profile in Fig. 6b, it is evident that most of the first 4 h are dominated by cluster 1 (one that matched on the two sides). In the last 2 h the trend is away from this cluster, towards a more suppressed EEG type (cluster 2). This record is severely abnormal, with markedly suppressed EEG and the change in the time profile appears to indicate worsening of the EEG.

The distribution (in terms of overall normality as determined by conventional reviewing) of the 41 6 h sections of EEG used in the validation of the AAS-EEG technique is as follows: 14 normal, 6 normal to mild, 8 mild, 3 mild to moderate, 7 moderate, 1 moderate to severe and 2 severe. In 3 of the 41 EEGs the AAS-EEG generated fewer than the desired number (5) of clusters; however, they were still considered in the validation. The validation results are presented in contingency Tables 2, 3, 4 and 5. Table 2 shows the overall assessment of the background; the validation results of the different attributes of the EEG (amplitude, symmetry and time variability) are presented in Tables 3–5. For the overall assessment of the EEGs, there was a 43.9% agreement with conventional EEG reviewing, 73.2% agreement within one-half level and a 100% agreement within one level. The agreement for amplitude was better than for overall assessment, for symmetry marginally better and for time variability marginally worse. The agreement results are summarized in Table 6. Only the time variability feature had a less than 100% agreement to within one level (7.3% agreement beyond one level).

4. Discussion

During most long-term monitoring procedures, there are extensive periods when the EEG is unchanging. When it is changing, it often fluctuates between a few different pat-

Table 3

Amplitude assessment

		Compressed EEG review						
		Norm	Norm-Mild	Mild	Mild-Mod	Mod	Mod-Sev	Sev
Conventional	Norm	15	0	2	0	0	0	0
EEG review	Norm-Mild	2	1	0	0	0	0	0
	Mild	1	1	3	3	0	0	0
	Mild-Mod	0	0	0	1	1	0	0
	Mod	0	0	1	2	3	2	0
	Mod-Sev	0	0	0	0	0	2	0
	Sev	0	0	0	0	1	0	0

Abbreviations: see Table 1.

Table 4
Symmetry assessment

		Compressed EEG review						
		Norm	Norm-Mild	Mild	Mild-Mod	Mod	Mod-Sev	Sev
Conventional	Norm	22	2	2	0	0	0	0
EEG review	Norm-Mild	5	0	0	0	0	0	0
	Mild	8	0	0	0	1	0	0
	Mild-Mod	0	0	0	0	0	0	0
	Mod	0	0	1	0	0	0	0
	Mod-Sev	0	0	0	0	0	0	0
	Sev	0	0	0	0	0	0	0

Abbreviations: see Table 1.

terns. We, therefore, felt that a method that could identify these patterns and provide their time distribution would give a ‘bird’s eye view’ of a long recording.

We have produced a method for summarizing prolonged EEG records — Automated Analysis of Segmented EEG (AAS-EEG) — that should allow clinicians to evaluate the normality of a record and identify any salient trends or acute changes relatively quickly. This method can be potentially employed with records of any duration using any number of channels. This contrasts with currently available EEG compression routines that work with only a limited number of channels for relatively limited periods of time (few hours in the case of CSA, or longer but with fewer channels for integrated amplitude displays). The output of the AAS-EEG method consists of two pages: the first demonstrates the main types of EEG present in the record, and the second shows the temporal distribution of the EEG types during the recording period. Unlike CSA or other such methods, our method presents actual EEG segments that are representative of the long recording. No new interpretive skill is therefore required: any person familiar with EEG can evaluate the results. The compact nature of the resulting display means that these few pages can easily be reviewed by a clinician at a remote site (for example at his or her home) using fax or modem. This information will allow the clin-

ician to quickly assess the background and identify any deterioration and thus come to timely decisions about care, and the urgency of the situation. It is important to remember, however, that it will not allow them to make a definitive diagnosis, nor to identify brief transient abnormalities such as infrequent seizures (although we have noted that in some cases seizures are clearly identified as a distinct EEG type using this method). Other methods are already available to identify these events. At a time when prolonged digital EEG recordings are providing invaluable but unwieldy amounts of data in the ICU setting, the AAS-EEG method has a clear role. This method is not intended to replace the standard EEG, but rather to allow a quick initial assessment of the background.

Our preliminary validation of the AAS-EEG method confirms that it provides the relevant clinical information required to make an assessment of background abnormalities. When asked to provide an overall assessment of the EEG, the evaluation by the reviewer using the AAS-EEG method agreed with the routine evaluation to within one level on the abnormality scale for all 41 6 h sections, and was within one half-level 73% of the time. When specific features of the EEG were assessed, similar agreement was reached with evaluation of amplitude and symmetry. The results obtained for time variability were slightly poorer,

Table 5
Time-variability assessment

		Compressed EEG review						
		Norm	Norm-Mild	Mild	Mild-Mod	Mod	Mod-Sev	Sev
Conventional	Norm	14	1	0	1	1	0	0
EEG review	Norm-Mild	2	0	0	1	0	0	0
	Mild	0	0	4	2	0	0	0
	Mild-Mod	0	0	0	1	4	0	0
	Mod	0	0	1	1	4	0	1
	Mod-Sev	0	0	0	0	0	0	0
	Sev	0	0	0	0	3	0	0

Abbreviations: see Table 1.

Table 6

Percentage agreement

	Overall	Amplitude	Symmetry	Time variability
% Agreement	43.9	61.0	53.7	56.1
% Agreement within 1/2 level	73.2	87.8	70.7	75.6
% Agreement within 1 level	100.0	100.0	100.0	92.7
% Agreement beyond 1 level	0.0	0.0	0.0	7.3

and reflect the reliance, during routine EEG review, on the identification of specific features, such as spindles and K complexes, which may not be apparent in the AAS-EEG. Another advantage of the AAS-EEG method, however, is that it provides information about gradual changes of the EEG. This is because it presents a summary of the EEG over long periods of time, and those data are difficult to appreciate when reviewing an EEG page by page.

The success of the AAS-EEG method depends on its ability to display examples that truly reflect the main types of EEG within a recording and demonstrate their distribution in time. Identification of characteristic EEG segments depends on many steps within the program, and we believe that the strength of the method lies in the details within each part of the algorithm. Many of the steps employed here have been reported in the literature in various attempts to analyze EEG signals; however, we are not aware of any study that has combined the methods in this way or analyzed prolonged EEG recordings. A fundamental component of the AAS-EEG method is the segmentation of the EEG into pseudo-stationary sections. Other attempts to segment EEG have met with limited success, either because they segment the EEG into sections of predetermined duration (and therefore ignore the boundaries of stationarity), or segment the EEG according to changes in only one feature. Most available methods use amplitude alone to determine segmentation; this ignores the clinically relevant role of frequency in the EEG. By using a novel measure of frequency-weighted energy, we have been able to incorporate frequency measures into our criteria for the segmentation of pseudo-stationary pieces of EEG. Thus far, we have applied this method to the independent segmentation of groups of channels on either side of the brain. We are currently examining the prospect of segmentation across all available channels simultaneously. This may simplify the temporal profile of the EEG types, without reducing any information in the EEG sample segments.

Having segmented the EEG in a way that makes sense from a clinical point of view, we then group all the segments into clusters according to how similar they are to each other. For this we use a variation on the *k-means* method. A major concern when trying to identify main EEG types is to determine how many natural clusters there are. This is a difficult problem, and we have addressed it by using an iterative type

of clustering algorithm and devising a novel way of ensuring an appropriate distribution of seed points. We have chosen to use a maximum of 5 clusters, some of which may be redundant when applied to invariant EEG records. If this is the case, it is trivial to allow the reviewers to recluster (with fewer clusters) based on their decision as to which clusters are redundant. By allowing the reviewers to decide for themselves we have, in part, resolved the issue of determining the number of natural clusters.

Another major component of the AAS-EEG method is the multi-level artifact rejection feature. Some effort was made to identify and reject artifacts at the level of the initial segmentation, and subsequently in clustering. This simplifies the review process and more closely mimics the behavior of the clinician.

Acknowledgements

We are grateful to Ms. Carol Leitner and the other staff of the EEG laboratory of the Montreal Children's Hospital for their collaboration. We are also grateful to Dr. R. Gottesman for his collaboration in the Pediatric ICU of the Montreal Children's Hospital. This work was supported in part by a grant from the Medical Research Council of Canada and Stellate Systems through the University-Industry program of the Medical Research Council (Grant MRC UI-11514).

References

- Amir, N. and Gath, I. Segmentation of EEG during sleep using time-varying autoregressive modeling. *Biol. Cybernet.*, 1989, 61: 447–455.
- Anderberg, M.R., 1973. *Cluster Analysis for Applications*. Academic Press, New York.
- Barlow, J.S., Creutzfeldt, O.D., Michael, D., Houchin, J. and Epelbaum, H. Automatic adaptive segmentation of EEGs. *Electroenceph. clin. Neurophysiol.*, 1981, 51: 512–525.
- Bickford, R., Fleming, N. and Billinger, T.W. Compression of EEG data. *Trans. Am. Neurol. Assoc.*, 1971, 96: 118.
- Bodenstein, G. and Praetorius, J.M. Feature extraction from the electroencephalogram by adaptive segmentation. *Proc. IEEE*, 1977, 65: 642–652.
- Bodenstein, G., Schneider, W. and Malsburg, C.V.D. Computerized EEG pattern classification by adaptive segmentation and probability-density function classification. Description of method. *Comput. Biol. Med.*, 1985, 15: 297–313.
- Borel, C., Hanley, D., 1985. Neurological intensive care unit monitoring. In: Rogers, M.C., Traysman, R.J. (Eds.), *Critical Care Clinics. Symposium on Neurological Intensive Care*. Saunders, Philadelphia, pp. 223–239.
- Bricolo, A., Turazzi, S., Faccioli, F., Sciaretta, G. and Erculiani, P. Clinical application of compressed spectral array in long term EEG monitoring of comatose patients. *Electroenceph. clin. Neurophysiol.*, 1978, 45: 211–225.
- Creutzfeldt, O.D., Bodenstein, G. and Barlow, J.S. Computerized EEG pattern classification by adaptive segmentation and probability-density-function evaluation. *Electroenceph. clin. Neurophysiol.*, 1981, 60: 373–393.
- Emmerson, R.G., Chiappa, K.H., 1988. Electrophysiologic monitoring. In:

- Ropper, A.H., Kennedy, S.K., Zervas, N.T. (Eds.), *Neurological Neurosurgical Intensive Care*, 2nd ed. Aspen, Rockville, MD, 1988.
- Gabor, A.J. and Seyal, M. Automated interictal EEG spike detection using artificial neural networks. *Electroenceph. clin. Neurophysiol.*, 1992, 83: 271–280.
- Gotman, J., Ives, J.R. and Gloor, P. Automatic recognition of interictal epileptic activity in prolonged EEG recordings. *Electroenceph. clin. Neurophysiol.*, 1979, 46: 510–520.
- Gotman, J. Automatic recognition of epileptic seizures in the EEG. *Electroenceph. clin. Neurophysiol.*, 1982, 54: 530–540.
- Harding, G.W. An automated seizure monitoring system for patients with indwelling recording electrodes. *Electroenceph. clin. Neurophysiol.*, 1993, 86: 428–437.
- Jordan, K.G. Continuous EEG and evoked potential monitoring in the neuroscience intensive care unit. *J. Clin. Neurophysiol.*, 1993, 10: 445–475.
- Kaiser, J.F., 1990. On a simple algorithm to calculate the ‘energy’ of a signal. In: *IEEE Int. Conf. Acoust., Speech, and Signal Processing*, Albuquerque, NM, April 1990, 1: pp. 381–384.
- Krajca, V., Petranek, S., Patakova, I. and Varri, A. Automatic identification of significant graphoelements in multichannel EEG recording by adaptive segmentation and fuzzy clustering. *Int. J. Biomed. Comput.*, 1991, 28: 71–89.
- Labar, D.R., Fisch, B.J., Pedley, T.A., Fink, M.E. and Solomon, R.A. Quantitative EEG monitoring for patients with subarachnoid hemorrhage. *Electroenceph. clin. Neurophysiol.*, 1991, 78: 325–332.
- Maynard, D.E., Prior, P.F. and Scott, D.F. Device for continuous monitoring of cerebral activity in resuscitated patients. *Br. Med. J.*, 1969, 4: 545.
- Pietela, T., Vapaakoski, S., Nousianinen, U., Varri, A., Frey, H., Hakkinen, V. and Neuvo, Y. Evaluation of a computerized system for recognition of epileptic activity during long-term EEG recording. *Electroenceph. clin. Neurophysiol.*, 1994, 90: 438–443.
- Plotkin, E.I., Swamy, M.N.S., 1992. Nonlinear signal processing based on parameter invariant moving average modeling. In: *Proc. CCECE '92*, Toronto, Canada, September 1992, pp. TM3.11.1–TM3.11.4.
- Sanderson, A.S. Hierarchical modeling of EEG signals. *IEEE Trans. Pattern Anal. Machine Intell.*, 1980, 2: 405–415.
- Ward, J.H. Hierarchical grouping to optimize an objective function. *Am. Stat. Assoc.*, 1963, 58: 236–244.
- Wendling, F., 1996. *Mise en correspondance d’observations EEG de profondeur pour la reconnaissance de signatures spatio-temporelles dans les crises d’épilepsie*. Ph.D. Dissertation, University of Rennes.
- Wertheim, D.F.P., Murdoch Eaton, D.G., Oozeer, R.C., Connel, J.A., Dubowitz, L.M.S., Dubowitz, V., Willetts, R. and Wootton, R. A new system for cotside display and analysis of the preterm neonate electroencephalogram. *Dev. Med. Child Neurol.*, 1991, 33: 1080–1086.
- Wertheim, D., Mercury, E., Faundez, J.C., Rutherford, M., Acolet, D. and Dubowitz, L. Prognostic value of continuous electroencephalographic recording in full term infants with hypoxic ischaemic encephalopathy. *Arch. Dis. Child.*, 1994, 71: F97–F102.